Θ State, Transition Curves, and Conformational Properties of Cyclic Chains

Ana M. Rubio and Juan J. Freire*

Departamento de Química Física, Facultad de Ciencias Químicas, Universidad Complutense, 28040 Madrid, Spain

Marvin Bishop

Department of Mathematics and Computer Science, Manhattan College, Riverdale, New York 10471

Julian H. R. Clarke

Department of Chemistry, University of Manchester Institute of Science and Technology, Manchester M60 1QD, U.K.

Received September 27, 1994[⊗]

ABSTRACT: We have performed a Monte Carlo study of dimensions and intrinsic viscosities for isolated three-dimensional cyclic chains of different lengths in solution. These chains are modeled as a number of Gaussian units interacting through a 6−12 Lennard-Jones potential. The reduced energy in the potential well represents the thermodynamic quality of solvent (or the reduced inverse temperature). From this study, the Θ state for this model has been characterized. Then, transition curves and scaling plots have been obtained. Using extrapolations to the long chain limit, different conformational parameters have been estimated and compared with existing experimental data.

Introduction

Cyclic polymers are systems of great theoretical interest. The preparation of synthetic ring polymers has made possible experimental investigations on the conformational properties of these molecules in dilute solution.[1,2] In order to interpret the data, one of the most fundamental areas of study has been the determination of the theta (Θ) state, i.e., the solvent conditions for which the binary interactions between chain units cancel out. Experimental data of intermolecular second virial coefficients for different ring polymer−solvent systems[3−6] have shown a depression in the Θ temperature of about 4−6 °C with respect to those corresponding to linear chains. Hence, this coefficient is positive at the Θ temperature of the linear polymer. However, different theoretical studies have pointed out[7,8] that a intermolecular repulsion between rings is expected in Θ solvents, due to the particular topological features of the rings. Therefore, it seems that, in contrast to linear chains, the Θ conditions cannot be characterized as those for which the second virial coefficient vanishes. Thus, the Θ point should be determined by the quasi-ideal behavior of conformational properties.

In the present work, we report a numerical study (Monte Carlo simulation) determining the Θ point for three-dimensional ring chains described by an off-lattice model.[9,10] Since a similar study has also been performed with the same model for linear chains,[11] it is interesting to analyze whether the ring topology alters the Θ conditions. Moreover, the determination of dimensions for other solvent conditions (excluded volume and sub-Θ, or collapse, regimes) allows us to plot transition curves. As we already know values of the properties for the homologous linear chains, ratios between ring and linear conformational properties are obtained in different solvent regimes; these ratios can be directly compared with experimental data. Although the determination of the Θ point is mainly based on the study of dimensions, we also obtain the intrinsic viscosity from a Monte Carlo average which provides a lower bound of this quantity,[12,13] free of the customary preaverage of hydrodynamic interactions.

Model, Monte Carlo Methods, and Averages

The model employed in this work was fully described and justified previously.[9,14] We consider N Gaussian units of root-mean quadratic length b (b is also the length unit in our calculations). Nonneighboring units interact through a 6−12 Lennard-Jones potential. The reduced distance at which the potential energy vanishes, σ/b, is set to the value $\sigma/b = 0.8$, which is chosen according to our experience in previous work with this model.[9,14] Then, the reduced energy in the well-depth of the potential, ϵ/k_BT, is the relevant parameter which determines the solvent conditions and can also be considered as a reduced inverse temperature.

The Monte Carlo methods employed in the present work are based upon the algorithms previously detailed for linear chains,[14] although we have introduced some particular features in order to deal with the ring architecture. First, we generate a closed nonoverlapping conformation on a diamond lattice. New conformations are generated from this starting state according to different algorithms depending on the solvent conditions we want to mimic:

(a) We randomly choose two chain units, i and j, and calculate the components of bond vectors $\mathbf{v}_i$ and $\mathbf{v}_{j+1}$ which connect these units to the longest part of the cyclic chain (see Figure 1). Then, we resample the components of both $\mathbf{v}_i$ and $\mathbf{v}_{j+1}$ from a Gaussian distribution with mean equal to zero and square deviation $b^2/3$, but keeping the same position vectors for units $i - 1$ and $j + 1$, $\mathbf{R}_{i-1}$ and $\mathbf{R}_{j+1}$. Consequently

$$\mathbf{R}_{i-1,j+1} = \mathbf{R}_{j-1} - \mathbf{R}_{i-1} \quad (1)$$

[⊗] Abstract published in *Advance ACS Abstracts,* February 15, 1995.

0024-9297/95/2228-2240$09.00/0

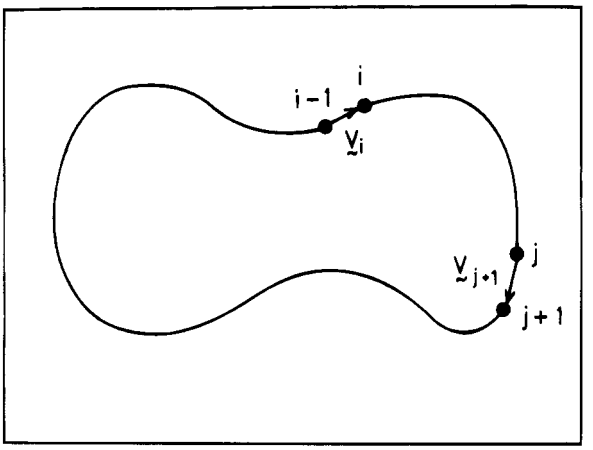

Figure 1. Notation for units and bond vectors along the ring chain.

has to be constant. Furthermore, we also maintain the difference vector between units i and j; i.e., $\mathbf{R}_{ij}$ is also fixed. We actually program this by keeping a constant sum $\mathbf{v}_i + \mathbf{v}_{j+1}$ and resampling the components of vector $\mathbf{v}_{j+1} - \mathbf{v}_i$ from a Gaussian distribution with mean equal to zero and square deviations $2b^2/3$. This way we calculate $\mathbf{v}_i$ and $\mathbf{v}_{j+1}$ and the new positions for units i and j. Finally, the shorter part of the chain between i and j is connected to these new positions (the longer one remains unaltered). Therefore, we perform a resampling of two bond vectors, followed by a translation of the shorter part of the chain to connect again with the changed units. This algorithm is efficient for chains in the Θ region. For the excluded-volume regime (i.e., for lower values of ϵ/k_BT so that the repulsive part of the potential is predominant) it is slightly more efficient to introduce a rotation of the shortest part of the chain around the axis defined by $\mathbf{R}_{ij}$, prior to its connection to the i and j units. This rotation is performed by an amount defined by the random angle ϕ. This latter procedure can be considered as a form of the pivot algorithm, known to be very efficient for the study of self-avoiding linear chains.[15]

(b) For chains in the sub-Θ temperature, i.e., for high values of ϵ/k_BT, we need to employ an algorithm with less drastic stochastic moves. Then, the new conformations are generated by changing a single unit, randomly chosen in each Monte Carlo step. Then, we use the same procedure explained in a, but set $i = j$. This single bead move for high ϵ/k_BT is identical to the one we used for linear chains[9,11,14] and, in fact, was the only one employed in previous simulations for rings with the present model, for all the different solvent regimes.[10,16]

The Metropolis criterion is used as a test for the acceptance or rejection of new conformations, according to the total Lennard-Jones intramolecular energy. We have verified that the results for dimensions (mean quadratic radius of gyration, $\langle S^2 \rangle$) obtained with two different sampling methods always overlap in the solvent regime intermediate between those for which these two methods are valid.

The averages are determined from eight independent runs. Therefore, we can estimate statistical means and uncertainties in a very simple way. The number of conformations attempted in each independent run depends greatly on the sampling method and the value of ϵ/k_BT. It varies from 40 000 (excluded-volume regime, pivot or translation algorithm) to 16×10^6 (lower range of the collapse region, single bead motion). We have tried to maintain uncertainties of $\langle S^2 \rangle$ within the range 1−2% of the mean value, for all the different cases. In each run, we disregard the first conformations ($1/6$ of the total number of attempts) to allow for an adequate thermalization. The final results for dimensions are contained in Table 1.

Table 1. Monte Carlo Results for Dimensions of Ring Chains of Different Lengths in Different Solvent Conditions

ϵ/k_BT	N	$\langle S^2 \rangle/b^2$	ϵ/k_BT	N	$\langle S^2 \rangle/b^2$
0.10	8	0.964 ± 0.007	0.40	8	0.8967 ± 0.0005
	19	2.728 ± 0.01		19	2.149 ± 0.004
	25	3.675 ± 0.005		25	2.75 ± 0.01
	37	6.00 ± 0.03		37	3.80 ± 0.02
	49	8.36 ± 0.09		49	4.63 ± 0.04
	55	9.65 ± 0.16		55	5.02 ± 0.05
	64	11.4 ± 0.3		64	5.45 ± 0.08
	80	14.86 ± 0.01		80	6.06 ± 0.09
	100	19.30 ± 0.02		100	6.52 ± 0.07
	124	24.86 ± 0.04		124	7.05 ± 0.07
	150	31.01 ± 0.07		150	7.81 ± 0.09
0.15	8	0.967 ± 0.001	0.45	8	0.8760 ± 0.0003
	19	2.665 ± 0.002		19	2.046 ± 0.002
	25	3.667 ± 0.005		25	2.547 ± 0.006
	37	5.77 ± 0.01		37	3.40 ± 0.02
	49	7.96 ± 0.02		49	3.97 ± 0.02
	55	9.04 ± 0.04		55	4.12 ± 0.02
	64	10.72 ± 0.04		64	4.49 ± 0.03
	80	13.96 ± 0.03		80	4.74 ± 0.03
	100	17.96 ± 0.02		100	5.01 ± 0.03
	124	23.01 ± 0.05		124	5.66 ± 0.03
	150	28.61 ± 0.02		150	6.52 ± 0.03
0.20	8	0.9570 ± 0.0007	0.50	8	0.85939 ± 0.00006
	19	2.582 ± 0.003		19	1.9383 ± 0.0007
	25	3.506 ± 0.006		25	2.367 ± 0.005
	37	5.44 ± 0.01		37	2.933 ± 0.009
	49	7.43 ± 0.03		49	3.32 ± 0.02
	55	8.44 ± 0.03		55	3.57 ± 0.02
	64	9.90 ± 0.04		64	3.62 ± 0.02
	80	12.75 ± 0.03		80	3.84 ± 0.01
	100	16.28 ± 0.04		100	4.34 ± 0.02
	124	20.58 ± 0.04		124	5.18 ± 0.01
	150	25.16 ± 0.07	0.55	8	0.8433 ± 0.0003
0.25	8	0.9448 ± 0.0007		19	1.827 ± 0.002
	19	2.478 ± 0.002		25	2.190 ± 0.002
	25	3.342 ± 0.005		37	2.554 ± 0.002
	37	5.08 ± 0.02		49	2.81 ± 0.01
	49	6.83 ± 0.02		55	3.124 ± 0.004
	55	7.66 ± 0.04		64	3.09 ± 0.01
	64	8.99 ± 0.06		80	3.419 ± 0.009
	80	11.25 ± 0.06		100	3.947 ± 0.002
	100	14.19 ± 0.05		124	4.22 ± 0.03
	124	17.40 ± 0.09	0.60	8	0.8262 ± 0.0002
	150	21.0 ± 0.1		19	1.708 ± 0.001
0.30	8	0.9314 ± 0.0007		25	2.008 ± 0.002
	19	2.374 ± 0.006		37	2.269 ± 0.005
	25	3.153 ± 0.009		49	2.489 ± 0.004
	37	4.68 ± 0.03		55	2.68 ± 0.01
	49	6.11 ± 0.04		64	2.740 ± 0.009
	55	6.88 ± 0.05		80	3.19 ± 0.01
	64	7.88 ± 0.06		100	3.47 ± 0.03
	80	9.58 ± 0.06			
	100	11.57 ± 0.06			
	124	13.8 ± 0.2			
	150	16.1 ± 0.1			
0.35	8	0.916 ± 0.001			
	19	2.265 ± 0.004			
	25	2.98 ± 0.01			
	37	4.21 ± 0.02			
	49	5.34 ± 0.04			
	55	5.96 ± 0.04			
	64	6.77 ± 0.06			
	80	7.66 ± 0.07			
	100	8.8 ± 0.1			
	124	9.9 ± 0.2			
	150	10.9 ± 0.3			

Table 2. Lower Bound Monte Carlo Averages of the Reduced Intrinsic Viscosity, $[\eta]^* = [\eta]M/Lb^3$ (L is Avogadro's Number), for Ring Chains of Different Lengths in Different Solvent Conditions

ϵ/k_BT	N	$[\eta]^*$	$\Phi \times 10^{-23}$	ϵ/k_BT	N	$[\eta]^*$	$\Phi \times 10^{-23}$
0.10	8	6.12 ± 0.06	2.64 ± 0.05	0.40	8	5.61 ± 0.04	2.71 ± 0.02
	19	29.7 ± 0.4	2.70 ± 0.05		19	22.5 ± 0.1	2.92 ± 0.03
	25	48.2 ± 0.8	2.69 ± 0.05		25	34.5 ± 0.2	3.10 ± 0.03
	37	99 ± 1	2.75 ± 0.05		37	60.2 ± 0.5	3.33 ± 0.05
	49	161 ± 5	2.7 ± 0.1		49	88 ± 1	3.6 ± 0.1
	55	200 ± 7	2.7 ± 0.2		55	100 ± 2	3.7 ± 0.1
	64	257 ± 7	2.7 ± 0.2		64	118 ± 1	3.8 ± 0.1
	80	364 ± 3	2.60 ± 0.02		80	157 ± 4	4.3 ± 0.2
	100	537 ± 3	2.60 ± 0.02		100	187 ± 5	4.8 ± 0.2
	124	783 ± 5	2.59 ± 0.02		124	224 ± 8	4.9 ± 0.3
	150	1102 ± 5	2.61 ± 0.02		150	272 ± 4	5.1 ± 0.2
0.15	8	5.90 ± 0.06	2.54 ± 0.03	0.45	8	5.6 ± 0.1	2.77 ± 0.05
	19	27.9 ± 0.1	2.62 ± 0.01		19	21.8 ± 0.1	3.05 ± 0.02
	25	44.9 ± 0.4	2.62 ± 0.02		25	32.2 ± 0.1	3.25 ± 0.02
	37	87.8 ± 0.5	2.60 ± 0.02		37	54.4 ± 0.2	3.56 ± 0.02
	49	148 ± 1	2.67 ± 0.03		49	75 ± 1	3.87 ± 0.05
	55	178 ± 2	2.68 ± 0.05		55	83 ± 2	4.07 ± 0.07
	64	226 ± 3	2.64 ± 0.05		64	98 ± 2	4.24 ± 0.07
	80	337 ± 2	2.64 ± 0.03		80	122.5 ± 0.5	4.86 ± 0.03
	100	494 ± 2	2.65 ± 0.01		100	149.9 ± 0.2	5.48 ± 0.02
	124	714 ± 3	2.65 ± 0.02		124	184 ± 3	5.59 ± 0.09
	150	1000 ± 1	2.68 ± 0.01		151	212 ± 3	5.22 ± 0.08
0.20	8	5.98 ± 0.06	2.62 ± 0.03	0.50	8	5.42 ± 0.01	2.786 ± 0.007
	19	27.1 ± 0.2	2.67 ± 0.02		19	20.7 ± 0.1	3.14 ± 0.02
	25	42.8 ± 0.3	2.67 ± 0.03		25	30.4 ± 0.1	3.42 ± 0.02
	37	85.2 ± 0.9	2.75 ± 0.04		37	47.7 ± 0.5	3.90 ± 0.04
	49	135 ± 1	2.71 ± 0.04		49	64.4 ± 0.5	4.38 ± 0.04
	55	165.2 ± 0.6	2.76 ± 0.02		55	73.3 ± 0.5	4.45 ± 0.03
	64	210 ± 3	2.76 ± 0.06		64	83.3 ± 0.1	4.96 ± 0.01
	80	311 ± 3	2.80 ± 0.04		80	102.7 ± 0.5	5.59 ± 0.03
	100	450 ± 3	2.81 ± 0.03		100	128 ± 3	5.8 ± 0.1
	124	638 ± 4	2.82 ± 0.03		124	150 ± 1	5.92 ± 0.03
	150	864 ± 6	2.81 ± 0.03	0.55	8	5.30 ± 0.04	2.80 ± 0.02
0.25	8	5.87 ± 0.04	2.62 ± 0.02		19	19.5 ± 0.1	3.23 ± 0.02
	19	26.2 ± 0.2	2.75 ± 0.02		25	27.8 ± 0.1	3.512 ± 0.006
	25	41.2 ± 0.3	2.76 ± 0.03		37	43.5 ± 0.2	4.36 ± 0.02
	37	78.6 ± 0.7	2.81 ± 0.04		49	56.4 ± 0.5	4.91 ± 0.04
	49	144.2 ± 0.7	2.84 ± 0.03		55	63.0 ± 0.3	4.68 ± 0.03
	55	149 ± 1	2.9 ± 0.5		64	72.0 ± 0.4	5.43 ± 0.03
	64	192 ± 3	2.92 ± 0.07		80	89 ± 2	5.8 ± 0.1
	80	273 ± 3	2.93 ± 0.06		100	105.1 ± 0.1	5.5 ± 0.1
	100	380 ± 4	2.97 ± 0.05		124	130 ± 1	6.13 ± 0.05
	124	542 ± 2	3.00 ± 0.03	0.60	8	5.25 ± 0.02	2.86 ± 0.01
	150	720 ± 3	3.05 ± 0.03		19	18.4 ± 0.1	3.38 ± 0.02
0.30	8	5.74 ± 0.06	2.62 ± 0.03		25	25.47 ± 0.04	3.669 ± 0.004
	19	25.1 ± 0.1	2.82 ± 0.03		37	38.2 ± 0.2	4.58 ± 0.03
	25	39.1 ± 0.4	2.86 ± 0.04		49	50.6 ± 0.5	5.28 ± 0.05
	37	71.8 ± 0.6	2.90 ± 0.05		55	55.8 ± 0.3	5.21 ± 0.03
	49	111 ± 2	3.05 ± 0.07		64	64.2 ± 0.4	5.79 ± 0.04
	55	138 ± 2	3.14 ± 0.08		80	77.6 ± 0.4	5.59 ± 0.03
	64	171 ± 2	3.17 ± 0.07		100	91 ± 2	5.8 ± 0.1
	80	233 ± 2	3.26 ± 0.07				
	100	321 ± 6	3.3 ± 0.2				
	124	438 ± 4	3.6 ± 0.2				
	150	551 ± 4	3.51 ± 0.08				
0.35	8	5.64 ± 0.05	2.63 ± 0.02				
	19	24.1 ± 0.1	2.89 ± 0.03				
	25	37.0 ± 0.3	2.95 ± 0.04				
	37	66.6 ± 0.5	3.17 ± 0.04				
	49	98.2 ± 0.6	3.27 ± 0.04				
	55	118 ± 2	3.3 ± 0.1				
	64	142 ± 3	3.3 ± 0.1				
	80	190 ± 2	3.68 ± 0.09				
	100	248 ± 4	3.8 ± 0.1				
	124	316 ± 8	4.2 ± 0.2				
	150	408 ± 2	4.7 ± 0.4				

The lower bound values of the intrinsic viscosity are obtained according to a variational method, first designed by Fixman[12] and fully described elsewhere.[13] These values are obtained as averages performed over a selected number of conformations randomly chosen from the whole Monte Carlo sample. (The calculations require one to compute a double sum of $3N \times 3N$ terms for each conformation.) Usually, we employ 3000 conformations for this purpose in each one of the independent batches. We introduce a parameter h^*, which describes the strength of hydrodynamic interactions between units. For this parameter, we used the previously employed value, $h^* = 0.25$, consistent with the definition of nondraining Gaussian units.[17] These lower bound averages represent an improvement with respect to the values one can obtain using the standard preav-

Table 3. Squared Deviations Δ and Slope v of the Fit to Equation 2 of Fitted Dimensions for Different Values of ϵ/k_BT (See Text)

ϵ/k_BT	$\Delta \times 10^3$	v	ϵ/k_BT	$\Delta \times 10^3$	v
0.230	4.4	0.512	0.240	1.2	0.500
0.232	3.7	0.510	0.242	1.0	0.498
0.234	3.0	0.508	0.244	1.2	0.495
0.236	2.3	0.505	0.246	1.6	0.492
0.238	1.7	0.503			

eraging of hydrodynamic interactions. Thus, previous results for Gaussian rings (i.e., without any consideration of intramolecular potential between units) show important differences (greater than 35%) between lower bound values and those obtained with the preaveraging approximation.[13] However, the differences are only about 10−15% between upper bound and lower bound results. (The upper bounds can be obtained through an alternative, though less efficient, method, based on evaluating the viscosity of conformations as rigid-body assemblies;[17] it requires the inversion of a $3N \times 3N$ diffusion matrix for each conformation.) The Monte Carlo lower bound results obtained with the present model and methods are shown in Table 2.

Θ-Point Determination

From the results for dimensions contained in Table 1, we have performed an analysis to determine the Θ point. This analysis has also been employed previously for data obtained with the same model of linear chains in two[18] and three[11] dimensions. It is essentially a simplified version of the method used by Meirovitch and Lim for lattice chain models.[19,20] After preliminary log−log linear fits to the scaling form

$$\langle S^2 \rangle^{1/2} \sim N^v \tag{2}$$

for each value of ϵ/k_BT we can make a rough assignment of the Θ region. According to Meirovitch and Lim, the Θ point should show the best correlation (flattest curve) in this type of fitting. However, we observe that correlation always decreases as ϵ/k_BT increases when the shortest chains are included in the analysis. (A similar problem was found in the study of linear chains[11] with the same model.) When we consider sufficiently long chains (apparently free of finite size effects), N = 80−150, we can delimit a low correlation range of values of ϵ/k_BT. In order to established more precisely the Θ-point location, the data corresponding to different values of ϵ/k_BT for a given chain length are fitted to a polynomial of the type

$$\ln \langle S^2 \rangle = a_0 + a_1 \ln(\epsilon/k_BT) + ... + a_n \ln(\epsilon/k_BT)^n \tag{3}$$

with $n = 4$ and 5. In this manner, we can obtain fitted dimensions for any temperature. After these fittings are carried out for all the different chain lengths, we divide the Θ region in intervals of width $\Delta(\epsilon/k_BT) = 0.01$, and employing the fitted dimensions obtained for the center of each interval and different chain lengths, we perform again the log−log linear fit to eq 2, obtaining correlations, squared deviations, and values of v as a function of ϵ/k_BT. As we previously stated, the Θ point is associated with the highest correlation (lower deviation).

The results for the deviations and the exponents v at the intervals closest to the Θ point are given in Table 3. From these results, we finally estimate the values

Table 4. Values of Φ Extrapolated to the Long Chain Limit, Together with Previous Numerical Estimations, and Results Obtained from Existing Experimental Data (See References 10 and 16)

ϵ/k_BT	$\Phi \times 10^{-23}$	ϵ/k_BT	$\Phi \times 10^{-23}$
0.10	2.60 ± 0.03	0.45	6.9 ± 0.1
0.15	2.74 ± 0.02	Gaussian chain,[a] preaveraged theory	5.23
0.20	2.83 ± 0.07	previous simulations	
0.25	3.18 ± 0.09	Θ region[b]	3.8 ± 0.2
0.30	3.8 ± 0.2	Excluded Volume[c]	2.8
0.35	5.0 ± 0.4	exptl data	
0.40	6.0 ± 0.5	Θ solvent	4.1,[d] 4.2[e]

[a] Reference 21. [b] Reference 10 (upper bound). [c] Reference 16 (upper bound). [d] Reference 4. [e] Reference 5.

$(\epsilon/k_BT)_\Theta = 0.242 \pm 0.002$ and $v_\Theta = 0.498 \pm 0.001$. It should be noticed that these results are pratically identical to those obtained for linear chains.[11] This seems to confirm that the Θ points for linear and ring chains are the same, even though the temperatures for which intermolecular second virial coefficients vanish are different.[2-6] We should also remark that the exponent v_Θ obtained through this method coincides with the one predicted by the mean-field theory (i.e., the well-known result for unperturbed Gaussian chains, $v_\Theta = 1/2$).

The reduced intrinsic viscosity values can also be analyzed in terms of the scaling law

$$[\eta]^* \sim [\eta]M \sim N^{v_\eta} \tag{4}$$

where v_η has to be $3/2$ for nondraining chains in the Θ point. (M is the chain molecular weight.) As in the case of linear chains,[11] however, we observe N-dependent v_η exponents, due to finite size effects, apparently more important for this conformational property. Also, we have investigated the parameter

$$\Phi = [\eta]^* M b^3 / 6^{3/2} \langle S^2 \rangle^{3/2} \tag{5}$$

which should depend weakly on the molecular weight. The values of Φ obtained from our dimension and viscosity simulation values for different chain lengths and fixed ϵ/k_BT have been included in log−log extrapolations vs N^{-1}, in order to estimate long chain limits for this parameter. These extrapolated values are included in Table 4, together with some previous numerical estimations and experimental data. A fitted interpolation of these values to the Θ point yields $\Phi = (3.16 \pm 0.08) \times 10^{23}$. This value is about 20% lower than the previous upper limit result,[10] obtained from calculations on shorter chains, using a preliminary estimation of the Θ point, $\epsilon/k_BT \simeq 0.3$. The experimental results[4,5] are also similarly higher than our value, though considerably smaller than the result obtained by the preaveraged theory.[21]

Transition Curves

Plots of dimensions vs reduced temperature for different values of N are presented in Figure 2. This way, we can clearly observe the transition from the excluded-volume regime (where the rings are expanded with respect to the Θ point dimensions) to the collapse regime. Obviously, the transition is less sharp than in the case of linear chains, which have significantly higher sizes in the Θ and excluded-volume regimes, and a similar collapsed form. According to the standard

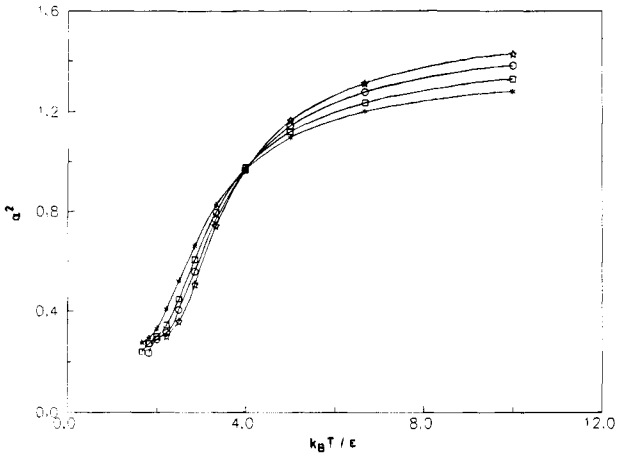

Figure 2. α^2 vs k_BT/ϵ (reduced temperature) for different chain lengths: (*) $N = 80$, (□) $N = 100$, (○) $N = 124$, (☆) $N = 150$.

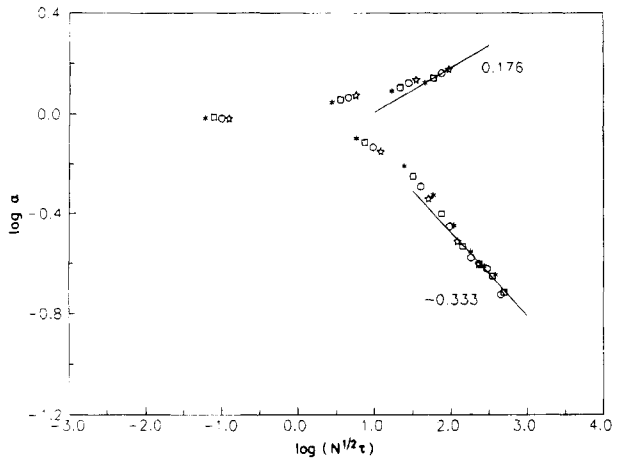

Figure 3. log–log plot of the expansion coefficient for the mean radius of gyration vs the absolute value of the scaling variable, defined by eq 6 with $\Phi_t = 1/2$. Numerical values for the plotted slopes correspond to the excluded-volume and collapsed regime limits, according to the values of υ_Θ and υ defined in text. Notation for chain lengths as in Figure 2.

scaling theory, these transitions can be described in the form of a universal curve for the expansion factor[22]

$$\alpha = (\langle S^2\rangle/\langle S^2\rangle_\Theta)^{1/2} \sim f[N^{\Phi_t}\tau] \tag{6}$$

where

$$\tau = |T - T_\Theta|/T_\Theta \tag{7}$$

$$f(z) = z^{(\upsilon-\upsilon_\Theta)/\Phi_t} \tag{8}$$

and $\Phi_t = 1/2$ for three-dimensional chains. Figure 3 contains a logarithmic scaling plot, which includes our results for different chain lengths and temperatures. The dimensions at the Θ point are interpolated from the fits described by eq 3. We also include the Figure 3 the expected slopes for the collapse ($\upsilon = 1/3$) and the excluded-volume ($\upsilon = 0.588$) limits. It can be observed that the chain-length variation for every temperature is in good agreement with theory for the data near each asymptotic regime. Moreover, there is a clear tendency of the different points to converge into a single universal curve as these limits are approached. Similar features were also observed for linear chains.[11] In Figure 4, we include the scaling plots for the viscosity data (defining

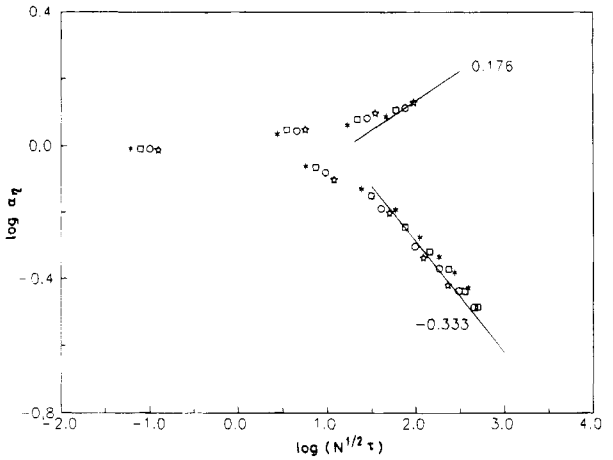

Figure 4. As in Figure 3, but for the viscosity expansion factor α_η.

a viscosity expansion factor $\alpha_\eta^3 = [\eta]/[\eta]_\Theta$). The curves also tend clearly to the expected limits, though finite size effects are more apparent for this property.

The parameter Φ values, obtained for the excluded-volume and collapse regimes, deserve also some attention. For the excluded-volume regime, $\epsilon/k_BT \simeq 0.1$, we find from the long chain extrapolations shown in Table 4 that $\Phi = (2.60 \pm 0.03) \times 10^{23}$. This result is close to (only about 10% smaller) the previous upper bound extrapolation[16] (obtained with shorter chains). It is also interesting to estimate the ratio between the parameter values obtained in the excluded-volume regime and the Θ point. We get $\Phi_{EV}/\Phi_\Theta = 0.82 \pm 0.04$, practically identical to the upper bound estimation,[16] close to our previous estimation for the linear chain[11] $\Phi_{EV}/\Phi_\Theta = 0.76 \pm 0.05$, and smaller than the approximate theoretical estimation for linear chains[23] $\Phi_{EV}/\Phi_\Theta \simeq 0.88$. For the collapse regime, we find much higher values of Φ, as the chain tends to be a compact structure. For a rigid sphere $\Phi = 9.23 \times 10^{23}$. The approach of the rings to this limit is faster than in the case of linear chains, since the ring constraints favor compact conformations.

Extrapolated Ratios

The ratio

$$q_s = \langle S^2\rangle_r/\langle S^2\rangle_l \tag{9}$$

between the ring dimensions and those of a linear chain of the same length (or molecular weight) can be evaluated from the present calculations and our previous results for linear chains.[11] (In some cases, the latter results for linear chains[11] have been used in interpolations to the required value of N.) The ratios for the Θ and excluded-volume regimes are extrapolated to the long chain limit (through linear regressions vs N^{-1}), and, then, they can be directly compared with experimental data. For the Θ point dimensions of both ring and linear chains, we use the fitted dimensions corresponding to $\epsilon/k_BT = 0.242$. The results for $\langle S^2\rangle_\Theta/N$ are appreciably larger than the value $1/12$ for Gaussian rings, due to the repulsive effects of three-body interactions. These differences with respect to the ideal chain have also been found in many other simulations for models including an intramolecular potential with an attractive term and are obviously larger for structures with a higher density of units (i.e., for stars[9] or rings[10] in comparison with linear chains[9,20]). A summary of the values for ratios q_s and q_n can be found in Table 5. For

Table 5. Ratios q_s and q_η, Extrapolated to the Long Chain Limit, Together with Previous Numerical Estimations and Experimental Data

	q_s	q_η
Θ region	0.521 ± 0.002	0.57 ± 0.01
excluded-volume region	0.54 ± 0.01	0.58 ± 0.01
Gaussian chain	0.5	0.66[a]
previous simulations		
Θ region[b]	0.57	0.60
excluded volume[c]	0.53	0.59
exptl data		
Θ solvents	0.53[d]	0.59,[d] 0.62,[e] 0.66,[f] 0.68[g]
good solvents	0.52,[d] 0.53,[g] 0.55[h]	0.56,[d] 0.66,[e] 0.72[i]
renormalization group theory (good solvents)	0.58[j]	0.56[k]
Brownian dynamics simulations (good solvents)	0.569 ± 0.036[l]	

[a] Preaveraged hydrodynamic interactions. [b] Reference 10. [c] Reference 16. [d] Reference 4. [e] Reference 27. [f] Reference 28. [g] Reference 5. [h] Reference 24. [i] Reference 29. [j] Reference 25. [k] Reference 29. [l] Reference 26 ($N = 64$). For further details on the estimation of the experimental ratios, see ref 10 (Θ solvents) and ref 16 (good solvents).

the Θ point, we obtain the value $q_s = 0.521 \pm 0.002$, close (though not identical) to the unperturbed Gaussian chain value, $q_s = 0.5$. Previous simulations for shorter chains for the same model[10] yielded $q_s = 0.57$. As previously stated, these simulations, however, were performed with the preliminary Θ point estimation, $\epsilon/k_BT = 0.3$ and, therefore, should reflect the expected closer similarity between rings and linear chains for more compact conformations. The present results yield $q_s = 0.54$ for the excluded-volume limit, very close to the one obtained in our previous Monte Carlo simulations[16] (same value of ϵ, $\epsilon/k_BT = 0.1$, but shorter chains). These estimations can be considered in good agreement with existing experimental data,[4,5,24] and they are close to those obtained from first-order renormalization group theory[25] and previous Brownian dynamics simulations based on a similar model.[26]

A similar analysis has been performed with the viscosity data. Thus, we have obtained the ratio between ring and linear chain viscosities

$$\Phi_\eta = [\eta]^r/[\eta]_l \qquad (10)$$

As we have already mentioned, the results for viscosity show finite size effects in the present range of chain lengths. Therefore, we have not employed them in an independent determination of the Θ point and use the value of $(\epsilon/k_BT)_\Theta$ evaluated from dimensions. However, with the exclusive aim of obtaining interpolated values for this Θ point, we have fitted the results for every chain length to a temperature dependence expression similar to eq 3

$$\ln([\eta]^*) = a_0 + a_1 \ln(\epsilon/k_BT) + ... + a_n \ln(\epsilon/k_BT)^n \qquad (11)$$

with $n = 4$ and 5. (Similar fits have also been performed with the results for the viscosity of linear chains, reported separately.[11]) The ratios both for the Θ point and the excluded-volume regime have been then extrapolated to the long chain limit. The results are also included in Table 5. For the Θ point, we get $q_\eta = 0.58$, close to the result obtained with the upper limit calculations for shorter chains.[10] As previously discussed,[10] the experimental data are extended over a wide range of values. Some of them[4,27] are about 0.60, but some others[5,28] are closer to 0.66, the theoretical result obtained by applying the approximate preaverage of hydrodynamic interactions to an unperturbed Gaussian chain. A wide dispersion of experimental data is also found for the excluded-volume regime.[4,27,29] In this case we have found $q_\eta = 0.58$, in agreement with the previous simulations[10] but slightly smaller than some of these experimental values. This result is also in agreement with first-order calculations based on the renormalization group theory.[30]

The two-parameter theory[2,31] for rings yields[32] α^2-(ring) $= 1 + (\pi/2)z + ...$ in terms of the excluded-volume parameter z. This can be compared with the result α^2-(linear) $= 1 + (134/105)z + ...$ Incorporating the different first-order coefficients, C_s, in z to the modified Flory equation for the excluded volume,[31] $\alpha^5 - \alpha^3 = C_s z$, one gets q_s/q_s(Gaussian chain) $= 1.23^{2/5}$, in the limit of large excluded-volume effects. This approach leads to $q_s \simeq 0.54$, consistent with our Monte Carlo results. For the viscosity, the perturbation result[2,31] is α_η^3(ring)/α_η^3-(linear) $= 1 + 0.04z + ...$, which indicates a small and positive z-dependence. This is consistent the comparison of our Monte Carlo values of q_η for the Θ and excluded-volume regions (both obtained with the same treatment of hydrodynamic interactions). Different approaches to large values of z with the same two-parameter theory[2,21,31,33] do not agree in providing a reliable value for q_η.

Concluding Remarks

We have determined the Θ point for an off-lattice model of isolated ring chains, using a criterion based in the highest correlation (flatest curve) for the fit of dimension data to eq 2. The value for this point is almost identical to that found for linear chains, investigated through the same model and method. We have performed transition and scaling plots, showing a good convergence of the data to the asymptotic excluded-volume and collapse universal regimes. Moreover, we have determined lower values of the intrinsic viscosity. These data show more significant finite size effects than the dimension results. However, the scaling plot for this property shows also a clear approach to the asymptotic limits. The ratios between dimensions (or viscosities) corresponding to a ring and a homologous linear chain in the Θ and excluded volume have been extrapolated to the long chain limit. Except in the case of ratio q_s at the Θ point, these ratios confirm previous results obtained with shorter chains, with a considerably different preliminary Θ point value (and corresponding to upper bound estimations of the intrinsic viscosity).

Acknowledgment. This research has been supported by Grant No. PB92-0227 of DGICYT (Spain), the NATO Collaborative Research Grants Programme (Grant No. CRG 911005), and the donors of the Petroleum Research Fund, administered by the American Chemical Society.

References and Notes

(1) Semlyen, J. A., Ed. *Cyclic Polymers*; Elsevier: London, 1986.
(2) Fujita, H. *Polymer Solutions*; Elsevier: Amsterdam, The Netherlands, 1990.
(3) Roovers, J.; Toporowski, P. M. *Macromolecules* **1983**, *16*, 843.
(4) Roovers, J. *J. Polym. Sci., Polym. Phys. Ed.* **1985**, *23*, 1117.
(5) Lutz, P.; McKenna, G. B.; Rempp, P.; Strazielle, C. *Makromol. Chem., Rapid Commun.* **1986**, *7*, 599.

(6) Hild, G.; Strazielle, C.; Rempp, P. *Eur. Polym. J.* **1983**, *19*, 721.
(7) Frank-Kamenetskii, M. D.; Lukashin, A. V.; Vologodskii, A. V. *Nature* **1975**, *258*, 398.
(8) Iwata, K. *Macromolecules* **1985**, *18*, 115.
(9) Freire, J. J.; Pla, J.; Rey, A.; Prats, R. *Macromolecules* **1986**, *19*, 452.
(10) García Bernal, J. M.; Tirado, M. M.; Freire, J. J.; García de la Torre, J. *Macromolecules* **1990**, *23*, 3357.
(11) Rubio, A. M.; Freire, J. J.; Clarke, J. H. R.; Yong, C. M.; Bishop, M. To be published in *J. Chem. Phys.*
(12) Fixman, M. *Macromolecules* **1983**, *78*, 1588.
(13) Freire, J. J.; Rey, A. *Comput. Phys. Commun.* **1990**, *61*, 297.
(14) Freire, J. J.; Rey, A.; Bishop, M.; Clarke, J. H. R. *Macromolecules* **1991**, *24*, 6494.
(15) Madras, N.; Sokal, A. D. *J. Stat. Phys.* **1988**, *50*, 109.
(16) García Bernal, J. M.; Tirado, M. M.; Freire, J. J.; García de la Torre, J. *Macromolecules* **1991**, *24*, 593.
(17) Zimm, B. H. *Macromolecules* **1980**, *13*, 592.
(18) Torres, A. M.; Rubio, A. M.; Freire, J. J.; Bishop, M.; Clarke, J. H. R. *J. Chem. Phys.* **1994**, *100*, 7754.
(19) Meirovitch, H.; Lim, H. A. *J. Chem. Phys.* **1989**, *91*, 2544.
(20) Meirovitch, H.; Lim, H. A. *J. Chem. Phys.* **1990**, *92*, 5144.
(21) Fukatsu, M.; Kurata, M. *J. Chem. Phys.* **1966**, *44*, 4539.
(22) des Cloizeaux, J.; Jannink, G. *Polymers in Solution. Their Modeling and Structure*; Clarendon Press, Oxford, U.K., 1990.
(23) Wang, S.-Q.; Douglas, J. F.; Freed, K. F. *Macromolecules* **1985**, *18*, 2464.
(24) Ragnetti, M.; Gaiser, D.; Höcker, H.; Oberthür, R. C. *Makromol. Chem.* **1985**, *186*, 1701.
(25) Prentis, J. J. *J. Chem. Phys.* **1982**, *76*, 1574.
(26) Bishop, M.; Saltiel, C. J. *J. Chem. Phys.* **1988**, *89*, 1159.
(27) He, Z.; Yuan, M.; Zhang, X.; Wang, X.; Jin, X.; Huang, J. *Eur. Polym. J.* **1986**, *22*, 597.
(28) Higgins, J.; Nicholson, L. K.; Hayter, J. B.; Dodgson, K.; Smelyen, J. A. *Polymer* **1983**, *24*, 793.
(29) Duval, M.; Lutz, P.; Strazielle, C. *Makromol. Chem., Rapid Commun.* **1985**, *6*, 71.
(30) Schaub, B.; Cramer, D. B.; Johanesson, H. *J. Phys. A: Math. Gen.* **1988**, *21*, 1431.
(31) Yamakawa, H. *Modern Theory of Polymer Solutions*; Harper and Row: New York, 1971.
(32) Casassa, E. F. *J. Polym. Sci.* **1965**, *A3*, 605.
(33) Bloomfield, V. A.; Zimm, B. H. *J. Chem. Phys.* **1966**, *44*, 315.

MA941227F